Available online at www.sciencedirect.com
ScienceDirect
Geochimica et Cosmochimica Acta 71 (2007) 3601–3615
Geochimica et Cosmochimica Acta
www.elsevier.com/locate/gca

Trace-element composition of Fe-rich residual liquids formed by fractional crystallization: Implications for the Hadean magma ocean

Cin-Ty Aeolus Lee [a,*], Qing-zhu Yin [b], Adrian Lenardic [a], Arnaud Agranier [a], Craig J. O'Neill [c], Nivedita Thiagarajan [a,d]

[a] Department of Earth Science, MS-126, Rice University, 6100 Main St., Houston, TX 77005, USA
[b] Department of Geology, University of California, Davis, One Shields Avenue, Davis, CA 95616, USA
[c] GEMOC, Department of Earth and Planetary Science, Macquarie University, NSW 2109, Australia
[d] Division of Geological and Planetary Sciences, California Institute of Technology, 1200 E. California Blvd, Pasadena, CA 91125, USA

Received 18 December 2006; accepted in revised form 23 April 2007; available online 3 May 2007

Abstract

New isotopic studies of ^{142}Nd, the daughter product of the short-lived and now extinct isotope ^{146}Sm, have revealed that the accessible part of the silicate Earth (e.g., upper mantle and crust) is more radiogenic in $^{142}Nd/^{144}Nd$ than that of chondritic meteorites. The positive ^{142}Nd anomaly of the Earth's mantle implies that the Sm/Nd ratio of the mantle was fractionated early in Earth's history and that the complementary low ^{142}Nd reservoir has remained isolated from the mantle since its formation. This has led to the suggestion that an early enriched reservoir, formed within Earth's first hundred million years (the Hadean), resides permanently in the deep interior of the Earth. One hypothesis for a permanently isolated reservoir is that there may be an Fe-rich, and hence intrinsically dense, chemical boundary layer at the core-mantle boundary. The protoliths of this chemical boundary layer could have originated at upper mantle pressures during extreme fractional crystallization of a global magma ocean during the Hadean but testing this hypothesis is difficult because samples of this early enriched reservoir do not exist. This hypothesis, however, is potentially refutable. Here, we investigate a post-Archean magnetite-sulfide magma formed by extreme magmatic differentiation to test whether residual Fe-rich liquids *of any kind* have the necessary trace-element signatures to satisfy certain global geochemical imbalances. The magnetite-sulfide magma is found to have high Pb contents (and low U/Pb ratios), high Re/Os ratios, and anti-correlated Sm/Nd and Lu/Hf fractionations. Permanent segregation of such a magma would (1) provide a means of early Pb sequestration, resulting in the high U/Pb ratio of the bulk silicate Earth, (2) be a source of radiogenic ^{187}Os in the source regions of plumes, and (3) provide an explanation for decoupled Hf and Nd isotopic evolution in the early Archean, which is not easily produced by silicate fractionation. However, the magnetite-sulfide magma is not highly enriched in K, and thus, at face value, this magma analog would not serve as a repository for all of the heat producing elements. Nevertheless, other Fe–O–S liquids reported elsewhere are enriched in apatite, which carries high concentrations of K, U and Th. Given some promising geochemical fractionations of the Fe-rich liquids investigated here, the notion of a Hadean Fe-rich residual liquid deserves continued consideration from additional experimental or analog studies.

1. INTRODUCTION

For some time, geochemists have largely believed that, except for small mass transfer associated with plumes rising from the deep mantle, convection in the Earth's upper and lower mantle are more or less physically separated. This

* Corresponding author. Fax: +1 713 348 5214.
E-mail address: ctlee@rice.edu (C.-T.A. Lee).

0016-7037/$ - see front matter © 2007 Elsevier Ltd. All rights reserved.
doi:10.1016/j.gca.2007.04.023

view was based on geochemical mass balance arguments, which indicated that the expected amounts of incompatible trace elements and noble gases could not be accounted for by summing up the amounts believed to be in the crust, uppermost mantle and atmosphere (Jacobsen and Wasserburg, 1979; O'Nions et al., 1979; Hofmann, 1988). The "missing" components have been thought to be sequestered in the primitive lower mantle (depths greater than 670 km). This view, however, was contested by geodynamicists, who showed that whole-mantle convection was physically more likely (Bunge et al., 1996). Convergence of ideas only began after subducting slabs were shown seismically to penetrate the transition zone, some perhaps descending to the core-mantle boundary (Grand, 1994; van der Hilst et al., 1997). Such observations require regular communication between the upper and lower mantle, making it more difficult (though not impossible) to sustain the notion of an isolated convecting upper mantle above the 670 km discontinuity.

While evidence for whole-mantle convection seems to be growing, the geochemical imbalances persist. How can the whole mantle convect while certain portions of the mantle do not get sampled in the uppermost mantle by mid-ocean ridges? New hypotheses for hidden reservoirs in the mantle have since been proposed to reconcile these seemingly inconsistent observations (Becker et al., 1999; Kellogg et al., 1999; Tolstikhin and Hofmann, 2005). One hypothesis receiving recent attention is that the region just above the core-mantle boundary is a long-lived chemical repository (Garnero, 2000; Tolstikhin and Hofmann, 2005). Seismologists have shown that there is a semi-global jump in seismic velocity (D''), 200–300 km above the core mantle boundary (Wysession et al., 1998). This, in turn, may be underlain by an ultra-low velocity zone (ULVZ), a 10–50 km thick layer immediately above the core-mantle interface and characterized by a ~10% drop in compressional wave velocity and a 20–40% drop in shear wave velocity (Garnero et al., 1998). While recent work suggests that D'' may in part be due to a post-perovskite phase change (Murakami et al., 2004; Wookey et al., 2005), others have entertained the possibility that D'' and/or the ULVZ may also have a compositional origin related to core-mantle reaction (Brandon and Walker, 2005), subduction of oceanic crust (Hofmann and White, 1982), partial melting (Williams and Garnero, 1996), primordial crustal differentiates from Earth's first hundred million years (Tolstikhin and Hofmann, 2005), or even subducted banded iron formations (Dobson and Brodholt, 2005). This paper concerns the nature of this putative chemical repository at the core-mantle boundary.

2. EARLY AND PERMANENT ISOLATION OF ENRICHED RESERVOIRS: A HYPOTHESIS NEEDING TESTING

The notion of a relatively isolated and enriched primordial reservoir at the core-mantle boundary has gained momentum due to recent neodymium isotopic studies. The accessible part of the Earth's mantle was shown to have anomalously high ^{142}Nd relative to the other Nd isotopes (e.g., high ^{142}Nd/^{144}Nd, where ^{144}Nd is stable Nd isotope having no radioactive parent), the former being a decay product of ^{146}Sm, a short-lived radio-isotope having a half-life of ~103 My (Boyet and Carlson, 2005). Due to the short half-life of ^{146}Sm, any primordial nucleosynthetic ^{146}Sm present at the time our solar nebula condensed should have decayed completely away within Earth's first 0.5 Gy. Barring the bulk Earth having a non-chondritic initial ^{142}Nd/^{144}Nd or Sm/Nd ratio, a high ^{142}Nd/^{144}Nd mantle requires extraction of a light rare-earth element (LREE) enriched reservoir (e.g., low Sm/Nd) from the mantle within the first ~30 My of Earth's accretion. However, to preserve this anomalous ^{142}Nd signature, this LREE-enriched reservoir must not have remixed back into the convecting mantle. One possibility for a LREE-enriched reservoir would be a very early crustal reservoir, but intact continental crust older than 3.96 Gy has not been preserved anywhere on the surface of the Earth. Boyet and Carlson (2005) suggested instead that this Hadean "crustal" reservoir must be stored in a relatively inaccessible part of the Earth's interior, one possibility being at the core-mantle boundary. This putative Hadean "crustal" reservoir was suggested to represent the very last liquid dregs of a crystallizing terrestrial magma ocean, which may have formed on Earth by the heat liberated from accretion and the late Moon-forming impact (Walter and Tronnes, 2004). Somewhat analogous to ideas about the lunar magma ocean (Hess and Parmentier, 1995), Boyet and Carlson (2005) suggested that the last dregs would be rich in Fe and highly incompatible trace elements, including the heat-producing elements K, U, and Th. They argue that its Fe-rich character would have rendered it negatively buoyant, allowing it to sink and reside permanently at the base of the mantle. Other recent studies have also hypothesized the existence of Fe-rich liquids during the Hadean (Tolstikhin and Hofmann, 2005).

Special circumstances are necessary to achieve appreciable levels of Fe-enrichment in the residual magmas. Early Fe-oxide crystallization (magnetite, spinel or ilmenite) must be suppressed during much of the differentiation process of magma because if this were not so, Fe would be rapidly removed from the evolving magma. Suppression of Fe-oxide crystallization requires fairly low oxygen fugacities because high oxygen fugacities would result in early saturation of Fe-oxide phases. If Fe-oxide crystallization can be suppressed, the crystallization of silicate minerals, such as olivine, pyroxenes and especially plagioclase, will drive derivative liquids to higher Fe contents because Fe is moderately to highly incompatible in this phases. Low oxygen fugacities are generally typical of the tholeitic differentiation series, which characterize mid-ocean ridge and intraplate settings. In contrast, magmas in calc-alkaline differentiation series evolve to higher oxygen fugacities (Osborn, 1959), possibly due to dissociation of water during emplacement into the crust (Lee et al., 2005). Thus, the majority of Fe-rich bodies found on Earth appear to be in the form of cumulates or residual liquids formed from extreme fractional crystallization along tholeiitic differentiation series (Bateman, 1951; Philpotts, 1967; McBirney, 1975; Ashwal, 1982; Jang et al., 2001; Jang and Naslund, 2003). Although very rare in calc-alkaline differentiation series, if low oxygen fugacities can exist locally, Fe-rich

liquids can occasionally form, such as in the northeastern Oregon part of the Cascades volcanic arc (Johnson et al., 2002).

Could large volumes of Fe-rich magmas have formed from a global Hadean magma ocean? In the case of the Hadean lunar magma ocean, this was almost certainly the case. The moon's low oxygen fugacity and lower magma ocean pressures would have, respectively, suppressed early oxide crystallization and enhanced plagioclase crystallization, yielding very Fe-rich derivative magmas. These conditions are probably responsible for the formation of the lunar anorthositic crust and the purported dense Fe-oxide layers at depth, the latter originating from the sinking of Fe-rich residual liquids during lunar magma ocean crystallization (Wood et al., 1970; Kolker, 1982; Stegman et al., 2003). In the case of Earth, oxygen fugacities may have been slightly higher than on the moon and the pressures associated with the Earth's early magma ocean were certainly greater (Carlson, 1994). Thus, extensive plagioclase cumulates probably did not form on Earth. This means that the degree of Fe-enrichment in the residual terrestrial magma ocean might have been less than that on the moon. Nevertheless, a residual Hadean Fe-oxide matte may have still formed on Earth because crystallization of olivine, pyroxene and lower mantle silicates (silicate perovskite) will also drive residual liquids to higher Fe contents. Given the incompatible nature of sulfur, many trace elements, and volatiles, extreme crystallization could have also generated a volatile-rich residual liquid containing Fe-sulfides and high amounts of incompatible trace elements (O'Neill, 1991b).

We are thus interested in testing whether a Fe-rich Hadean matte formed and now resides permanently at the Earth's core-mantle boundary, serving as one of the missing reservoirs for various trace element imbalances. This hypothesis can be tested (e.g., potentially refuted) by constraining the trace-element composition of the putative missing reservoir, but unfortunately, we are unlikely to ever sample such material directly. As such, all constraints on its composition have been based on indirect mass balance arguments (Boyet and Carlson, 2005).

One way to test this hypothesis is to examine analog systems for inconsistent or consistent observations. These analog systems can be investigated using laboratory experiments, natural analog experiments, or theoretical experiments. The value of each experiment depends on how reasonable the experimental conditions match the real scenario. Laboratory and theoretical experiments have the advantage that one can control the experimental setups to match the first-order variables and conditions of the real scenario. This, of course, requires that one has a reasonable understanding of how the real scenario works and this may or may not be the case. The alternative is to use a geologically recent natural analog system, which may incorporate many of the complexities of the real Hadean scenario. However, the drawbacks are that (1) the geologically recent analog may not be perfectly analogous to Hadean scenarios and (2) the inherent complexities may make it more difficult to understand what is truly going on.

There is thus no perfect way to test this hypothesis. We have chosen the natural analog approach as a first step. Here, we investigate the trace-element composition of a Proterozoic Fe-oxide–sulfide magma (Fe–O–S magma), which represents the product of extreme magmatic differentiation, albeit at a much shallower level than the putative Hadean magma ocean. This Proterozoic outcrop is clearly not a perfect analog for the Hadean magma ocean because of its shallow origin. However, its composition (Fe, O, S) may be similar to that of the Hadean matte. Our objective here is to simply ask whether Fe–O–S type magmas are capable of generating any trace-element fractionations whose sense may help explain various geochemical "paradoxes" relevant to the Earth's mantle.

3. ONE TEST OF THE HYPOTHESIS: PROTEROZOIC MAGNETITE-SULFIDE MAGMAS

3.1. Composition

Our investigation is centered on an iron oxide/sulfide ore complex just north of the Kingston ranges in southeastern California (Hewett, 1948; Calzia et al., 1988). The ore complex (Fig. 1) is associated with 1.08 Gy diabases (Heaman and Grotzinger, 1992) intruded into neo-Proterozoic dolomites and limestones in the Crystal Springs Formation, well-exposed near Beck Springs (N 35° 47′26.6″, W 115° 56′ 22.7″). Both the diabase and Fe oxide/sulfide ores occur as stratiform sills within carbonate sedimentary beds, which have since been tilted nearly vertically (Fig. 1). In a previous study of these ores (Hewett, 1948), it was suggested that the ores were formed by contact metamorphism of carbonates by the Kingston Peak pluton. Indeed, a number of studies have shown an association of magnetite ores with limestone skarns formed by granitic or granodioritic plutons (Einaudi and Burt, 1982). However, this scenario does not appear to be the case because the Kingston Peak granites are 13 My old (Calzia et al., 1988) and granitic/rhyolitic dikes associated with the Kingston peak pluton crosscut both the diabase and the Fe-oxide ores. Instead, the ores are most likely petrogenetically related to the diabase sills (Calzia et al., 1988). Diabase sills are found within 5–50 m on both sides of the Fe oxide/sulfide sills. In addition, intermingling of diabase and Fe oxide/sulfides are exposed in a nearby open-pit mine. These observations indicate that the Fe oxide/sulfide sills ultimately derive from the diabase. The fluids associated with the Fe-oxide/sulfide sills could have derived from late stage exhalation of the diabase sills (Calzia et al., 1988) or possibly even from the sedimentary country rock (Barton and Johnson, 2000). Below, we discuss the petrography and geochemistry of these Fe oxide/sulfide sills and show that the trace element fractionations of interest are internal to the Fe-oxide/sulfide and diabase complex and hence not related to any external derivation of fluids.

The Fe oxide/sulfide ores can be subdivided into two groups. One group is characterized by cumulate layers of euhedral magnetite crystals and a Mg-silicate mineral, now altered primarily to chlorite (sulfides are absent). These cumulate layers are in close association with the diabase sills and are represented by two samples (Tal and BSNEB; see Table 1). This group is referred to as the Fe-oxide cumulates or Fe–O cumulates. The other group shows no textural evidence of a cumulate origin and is composed of ~90% massive

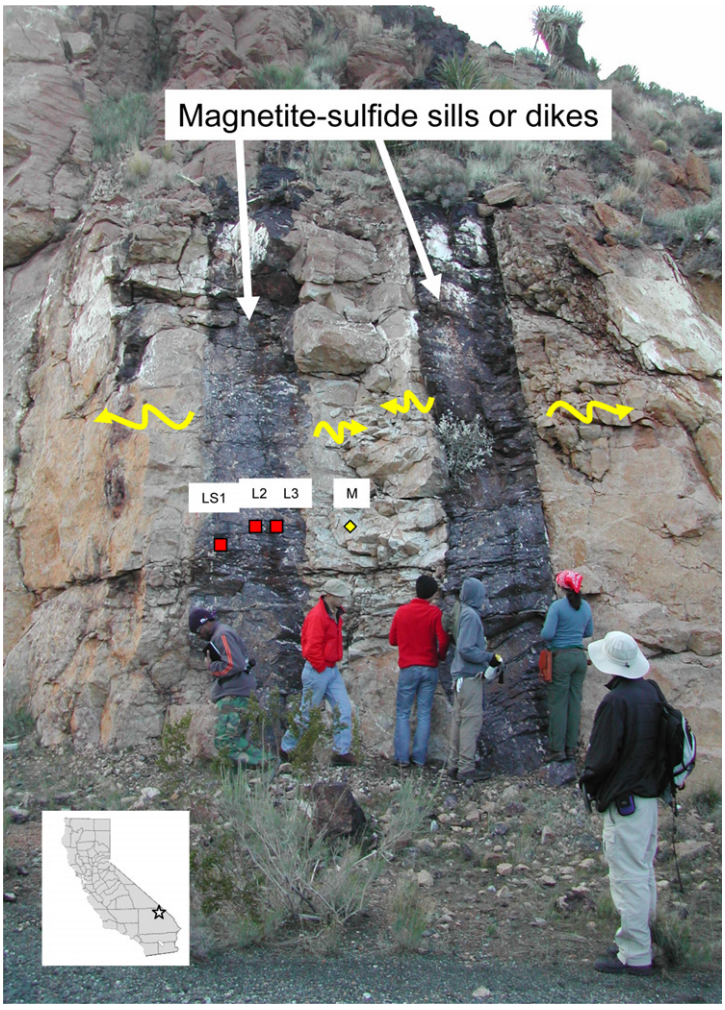

Fig. 1. Magnetite-sulfide (Fe–O–S) magmas intruded as sills in Proterozoic limestones of the Crystal Springs Formation in southeastern California (location shown in map inset); beds have been tilted vertically. Sample names are shown (Fe–O–S sills are "LS1", "L2", and "L3"; metasomatized carbonate is "M"). Central zone is not shown in photo. Sedimentary beds have since been tilted nearly vertically. Yellow arrows show the extent of cryptic trace-element metasomatism imparted by infiltration of a fluid component from the Fe–O–S sills and consequent loss of trace elements to the environment from the sills themselves. (For interpretation of the references to colour in this figure legend, the reader is referred to the web version of this article.)

Table 1

		Wallrock carbonate M	Fe–O–S sill (magagnetite-sulfi de)			Fe–O cumulate (magnetite)		Chondrite[a]	BCC[b]
			LS1	L2	L3	BSNEB	Tal		
Sm/Nd	Weight ratio	0.26	0.22	0.24	0.22	0.36	0.36	0.33	0.20
U/Pb	Weight ratio	0.11	0.01	0.01	0.005	1.45	1.84	0.14	0.11
Lu/Hf	Weight ratio	0.88	1.75	0.60	0.61	0.12	0.05	0.24	0.09
Re/Os	Weight ratio							0.08	13
Re/190Os	Weight ratio		529	340	22.2	15.4	43.6	0.31	50
$^{187}Re/^{188}Os$	Atomic ratio		2540	1633	107	74	209	0.39	64
Pt/Os	Weight ratio							2.06	50
$Pt/^{190}Os$	Weight ratio		23	1.3	1.3	4.8	4.2	7.82	190
$^{190}Pt/^{188}Os$	Atomic ratio		0.45	0.27	0.026	0.093	0.082	0.149	0.587

[a] Chondrite from Anders and Grevesse (1989).
[b] BCC, upper continental crust from Rudnick and Gao (2004).

crystalline magnetite, ~10% Fe sulfides (chalcopyrite and pyrite) and little or no silicates (LS1, L2, and L3; Fig. 1). The second group will be herein referred to as the magnetite-sulfide sills (Fe–O–S sills) and forms the focus of this paper. Apatite and ilmenite were not observed in either group. Interestingly, the diabase sills have resulted in local contact metamorphism of the carbonates as evidenced by marbleized contacts containing talc, tremolite, and serpentine mineralization. In contrast, intrusion of the Fe–O–S sills did not recrystallize adjacent carbonates into marble (although the carbonates have been extensively metasomatized by fluids from the Fe–O–S sills as discussed below); under thin section, the carbonate wallrock preserves original sedimentary textures, suggesting that the temperature of the magnetite-sulfide sills was significantly cooler than that of the diabase itself.

The two lithologic groups (the Fe–O cumulates and the Fe–O–S sills) have similar major element compositions, being characterized by 60–70 wt% total FeO (see Table 1). TiO_2 (<0.03 wt%) and P_2O_5 (<0.01 wt%) contents in both groups are extremely low, consistent with the lack of visible ilmenite and apatite in thin section. Analytical details and trace element compositions of the two lithologic groups are shown in Appendix A. Select trace element ratios are shown in Table 1. All of the magnetite samples are characterized by enrichments in U, Th, and Pb and depletions in Eu and Ni (Fig. 2a). The latter depletions suggest extensive fractionation of plagioclase and ultramafic minerals, such as olivine and pyroxenes. Plagioclase crystallization would also impose a negative Sr anomaly, but the Sr contents in these magnetites may have been partly compromised by secondary contamination of late-stage cross-cutting calcite

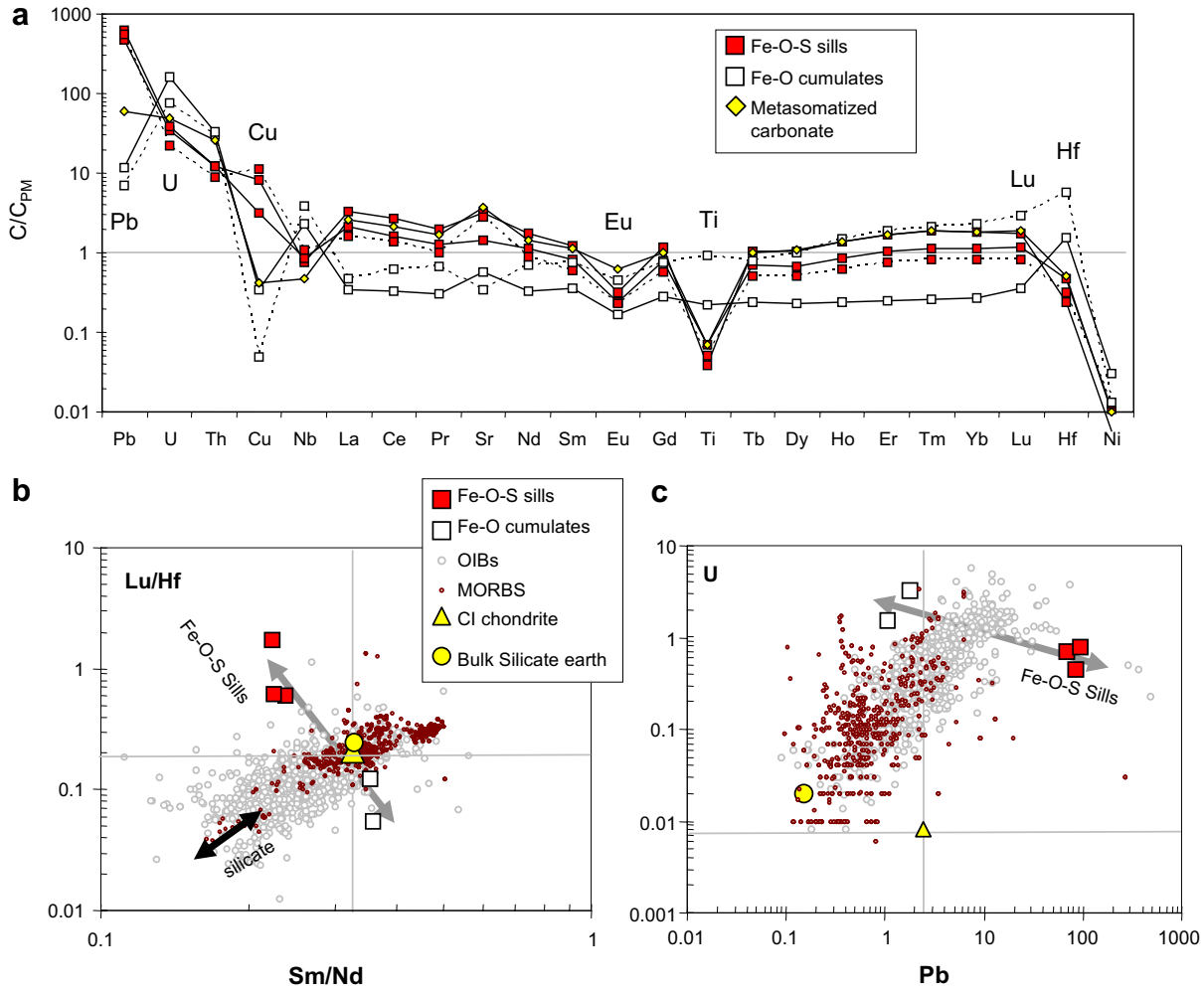

Fig. 2. (a) Primitive-mantle normalized (McDonough and Sun, 1995) trace-element abundances of the magnetite bodies; filled red squares correspond to the Fe–O–S sills shown in Fig. 1, which are taken here to provide a window into the trace-element composition of the putative Hadean Fe–O–S matte; open squares correspond to the cumulate magnetites (Fe–O cumulates), which contains only Fe-oxide and no sulfide. (b) Whole-rock Lu/Hf versus Sm/Nd of the Fe–O–S sills (red filled squares) and Fe–O cumulates (open squares). Also plotted are ocean island basalts (OIBs) and mid-ocean ridge basalts (MORBs) from the literature to show the effect of silicate differentiation. Black arrowed line shows how Lu/Hf and Sm/Nd are fractionated by silicate processes while the gray arrow shows the effect of Fe–O–S fractionation. (c) Whole-rock U verus Pb concentrations with symbols identical to b. Gray arrow shows the effect of Fe–O–S fractionation. Estimates of bulk silicate Earth and CI chondrite compositions are shown in (b) and (c). (For interpretation of the references to colour in this figure legend, the reader is referred to the web version of this article.)

veins. The two groups differ in that they have roughly complementary trace element signatures (Fig. 2), indicating their cogenetic relationship. The Fe–O–S sills are characterized by high light rare-earth element (LREE) to heavy rare-earth element (HREE) ratios, low Lu/Hf ratios, high Cu, high Pb contents and low U/Pb ratios. The cumulate layers are characterized by LREE depletion, high Lu/Hf, low Cu, low Pb, and high U/Pb, and hence show complementary fractionations to the Fe–O–S sills. The high Cu and Pb and low U/Pb of the Fe–O–S sills are consistent with the presence of sulfides and the chalcophile nature of Cu and Pb (the opposite is true for the central zone, which is devoid of sulfide).

The Fe–O–S sills have trace-element signatures requiring extreme plagioclase fractionation at some point prior to their emplacement. In addition, the parental magma must also have had a relatively low oxygen fugacity. These properties are consistent with the Fe–O–S sills originating from the diabase sills rather than from more oxidized partial melts of pre-existing crust (e.g., granites) or hydrothermal alteration of pre-existing crust. However, unlike magnetite and ilmenite bodies in layered mafic intrusions, which are mostly cumulates, the magnetite-sulfide sills represent quenched or fully crystallized Fe–O–S fluids.

A fluid nature to the Fe-oxide/sulfide sills could explain the fractionation of various incompatible trace elements. Magnetite crystals alone do not hold high concentrations of trace elements (Horn et al., 1994), but a Fe–O–S fluid/melt can. We examined the trace-element signature of neighboring carbonate beds (sample 'M' in Fig. 1) and found that their trace-element signatures roughly parallel that of the sills despite the fact that their major element composition (except for a slight enrichment in Fe) has not been changed appreciably. This confirms that most of the trace elements are probably not in the magnetite crystals but rather in a separate fluid phase that forms an interstitial component in the magnetite-sulfide sills and has, to a large extent, been expelled into the surrounding country rock as evidenced by the cryptically metasomatized carbonates (Figs. 1 and 2). Due to infiltration into the country rock, the absolute abundances of trace-elements in the magnetite-sulfide magma prior to emplacement were probably much higher than what we measure now in the sills. Extreme fractional crystallization may have thus resulted in the formation of a fluid/melt considerably enriched in Fe-oxides, sulfides *and* highly incompatible trace elements. Not all incompatible trace elements, however, appear as measured enrichments. Elements, such as K, Na, and Cs, which are normally considered to be highly incompatible are in low abundance in the magnetites and in the carbonate wallrock. Either these elements were never partitioned into the magnetite-sulfide magmas or they were subsequently leached out by weathering or low-grade metamorphism owing to their high aqueous solubilities.

3.2. A comment on wallrock contributions to trace elements

In Section 4, we will discuss whether the trace element characteristics of the Fe–O–S sills can resolve some outstanding global geochemical imbalances, but before doing so, it is necessary to address whether the observed trace-element fractionations are a result of igneous fractionation processes or the result of contamination by fluids mobilized from the wallrock sediments. While there is indeed evidence for considerable contact metamorphism of the limestones adjacent to some of the diabase sills (Calzia et al., 1988), the unusual trace-element fractionations in the Fe–O–S sills have anything to do with contact metamorphism. The strongest line of evidence against a sedimentary or metamorphic source to the unusual fractionations in the Fe–O–S sills is that the trace element fractionations in the Fe–O–S sills have complementary counterparts in the Fe–O cumulates (Fig. 2). The Fe–O–S sills have high Lu/Hf, low Nb/La, low U/Pb, and low Sm/Nd, which are complemented by the low Lu/Hf, high Nb/La, high U/Pb, and high Sm/Nd ratios of the Fe–O cumulates. Thus, the trace-element fractionations in the Fe–O–S sills that we will discuss in the next section clearly resulted from internal igneous differentiation processes. As for the source of the fluids themselves, they could be derived from sedimentary country rock (Barton and Johnson, 1996) or from hydrothermal fluids released from the diabase sill itself (Menard, 1995), but because the trace-element fractionations are internal to diabase and Fe-oxide/sulfide complex, the origin of the fluids is not critical to our study.

4. CAN FE-RICH MAGMAS RESOLVE ANY GEOCHEMICAL IMBALANCES?

Magnetite and Fe-sulfides are so much denser than mantle silicates that a residual Hadean liquid having a composition similar to our Proterozoic Fe–O–S sills would have sunk rapidly to the bottom of the mantle (Fig. 3a and b). This material might also be expected to remain at the bottom of the mantle indefinitely. Using the third order Birch–Murnaghan equation of state (see Appendix A and references in (Bina and Helffrich, 1992)) and the appropriate thermodynamic properties of magnetite (Fei, 1995; Haavik et al., 2000; Reichmann and Jacobsen, 2004), the density of magnetite at the core-mantle boundary (135 GPa, 3000 K; Boehler et al., 1995) is $\sim$7200 kg/m^3, which is $\sim$30% higher than the PREM density (5491 kg/m^3) of the silicate mantle just above D'' (Dziewonski and Anderson, 1981). This compositional density contrast is far greater than any plausible temperature-induced buoyancies ($\sim$1000 K) across the thermal boundary layer at the core-mantle boundary (Boehler et al., 1995). This increase in density would be reduced if the magnetite mixed or reacted with silicates. However, the effect of Fe-enrichment on density is so strong that the general conclusion remains unchanged.

We now ask what long-term geochemical signatures could be imposed on the Earth's mantle if a Hadean matte, having trace-element compositions similar to our Proterozoic Fe–O–S sills, was permanently sequestered at the bottom of the mantle? We are essentially concerned with whether the sense of fractionation imparted by Fe–O–S magmas is even in the correct direction to explain various geochemical imbalances. Our discussion thus focuses on trace-element ratios. Table 1 shows the trace element ratios of interest determined on our Fe-oxide/sulfide samples

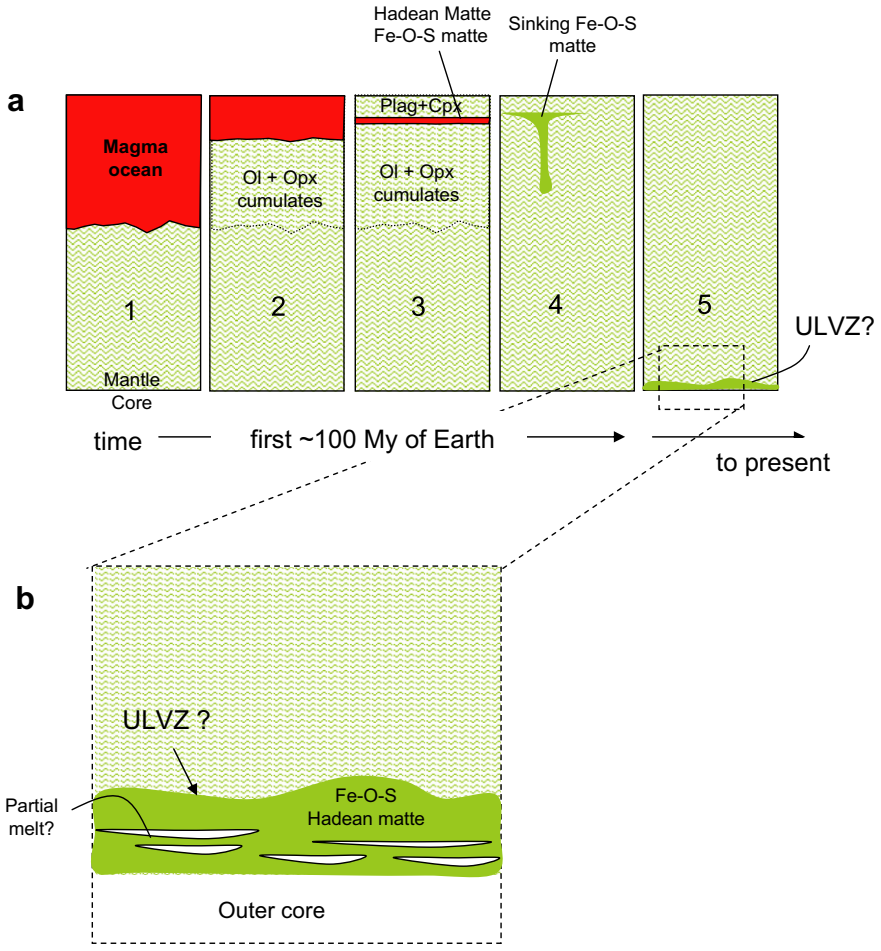

Fig. 3. (a) Cartoon of the cooling/crystallizing magma ocean and the generation of a Hadean Fe–O–S matte, followed by its catastrophic removal to the core-mantle boundary in the first ~100 My of Earth's history (steps 1–4). The Fe–O–S matte remains stable at the core-mantle boundary indefinitely and is hypothesized here to define the ultra low velocity zone (ULVZ). (b) Enlarged view of the core-mantle boundary and the Hadean Fe–O–S matte. The lower part may also undergo partial melting to generate a sulfide-rich melt.

(details in Appendix A) along with the corresponding ratios for continental crust (Rudnick and Gao, 2004) and chondrite (Anders and Grevesse, 1989). Our emphasis on ratios is further motivated by the fact that the absolute abundances of trace-elements in our Fe–O–S magmas are minimum estimates because much of the trace elements have been expelled (without significant fractionation since the cryptically metasomatized carbonate wallrock has roughly the same relative trace-element signature as the Fe–O–S magmas) from the sills themselves and forced into the carbonate country rock. Because we do not know how much fluid mass has been expelled into the country rock, our constraints on the original absolute concentrations are poor.

4.1. Decoupling of Sm/Nd and Lu/Hf

The low Sm/Nd of the Fe–O–S sills (Fig. 2b) implies that sequestering such material at the core-mantle boundary would impose a high Sm/Nd ratio on the residual silicate part of the Earth, allowing the silicate Earth to evolve towards a positive $^{142}Nd/^{144}Nd$ anomaly with respect to the chondritic Sm/Nd ratio the Earth is thought to have originated from. The sills moreover have low Sm/Nd but high Lu/Hf (Fig. 2b). The observed anti-correlation between Sm/Nd and Lu/Hf ratios is opposite that expressed by most terrestrial rocks—differentiation processes involving upper mantle silicates yield positive correlations between Sm/Nd and Lu/Hf (Fig. 2b) as exemplified by positive correlations of $^{143}Nd/^{144}Nd$ and $^{176}Hf/^{177}Hf$ isotopes in basalts (Vervoort and Patchett, 1996; Blichert-Toft and Albarède, 1997) (the strongly correlated fractionation of Sm/Nd and Lu/Hf is shown schematically as the thick red line in Fig. 4). However, one paradox has been that early Archean (3.96 Gy) rocks from Isua, Greenland already show positive deviations in $^{143}Nd/^{144}Nd$ (^{143}Nd is the decay product of ^{147}Sm, a longer-lived isotope of Sm) relative to chondrite but little to no concomitant anomaly in $^{176}Hf/^{177}Hf$ (Bennett et al., 1993; Bowring and Housh, 1995; Vervoort and Blichert-Toft, 1999; Bennett, 2003; Bizzarro et al., 2003; Caro et al., 2005). This requires that the Hadean upper mantle (blue ovals in Fig. 4) be characterized by high Sm/Nd (e.g., light rare-earth depleted) but near-chondritic Lu/Hf ratio. As shown schematically in Fig. 4, the bold red line characterizing upper mantle silicate differentiation ("normal mantle differentiation") must have been rotated clockwise in Lu/Hf versus Sm/Nd space during

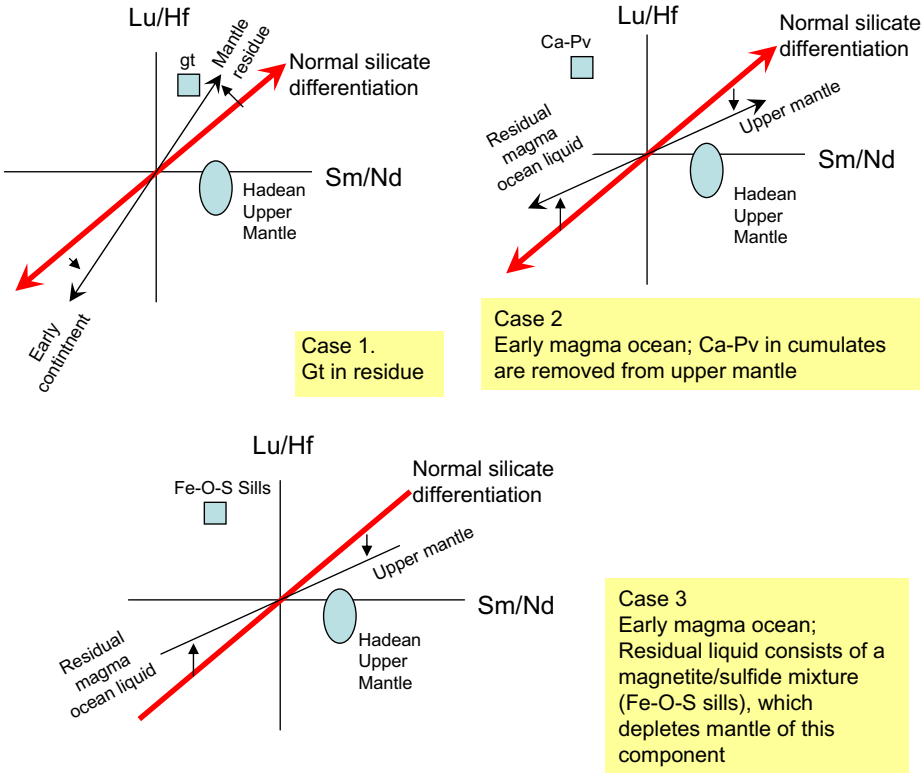

Fig. 4. Cartoon showing the effects of various fractionating phases (squares) on the evolution of Sm/Nd and Lu/Hf in the upper mantle. Axes are Lu/Hf (vertical) and Sm/Nd (horizontal). The axes represent relative deviations from a common starting point (presumably chondritic mantle), which is where the two axes cross. Bold red line represents typical differentiation trend that the upper mantle would follow if all fractionation was controlled by shallow pressure silicates (spinel peridotite). Melts (or continental crust) should plot in lower left hand quadrant while mantle residuum plots in the upper right hand quadrant. Unusual fractionating phases will cause the thick red line to rotate, that is, the upper mantle differentiation trend will be perturbed. Case 1 considers the scenario in which garnet is in the residual mantle during melting. This causes the residual mantle to have slightly higher Lu/Hf for a given Sm/Nd, hence the mantle array rotates counter-clockwise. Case 2 considers the magma ocean scenario in which Ca-perovskite accumulates in the lower mantle (Caro et al., 2005), which because of its high Lu/Hf ratio, results in an upper mantle with low Lu/Hf for a given Sm/Nd. This causes a clockwise rotation of the mantle array. Case 3 also considers a crystallizing magma ocean, except in this case, the residual liquid has a magnetite component having high Lu/Hf akin to the Fe–O–S magmas in this study. Sequestration of this Fe-rich residual liquid at the core-mantle boundary would leave behind a mantle having low Lu/Hf, driving a clockwise rotation. The Hadean upper mantle (blue oval in all panels) is believed to have low time-integrated Lu/Hf and superchondritic Sm/Nd, hence only those cases that result in a clockwise rotation of the mantle array are viable. (For interpretation of the references to colour in this figure legend, the reader is referred to the web version of this article.)

Hadean times if the apparent decoupling of Hf and Nd in the Isua rocks is real. From Fig. 4, it is clear that sequestering an early crust formed by melting of the mantle with garnet in the residual mantle causes the thick red line to rotate counter clockwise, moving the residual mantle *away* from the Isua mantle. What seems required is a fractionating phase that lies in the upper left hand quadrant of the diagrams in Fig. 4, that is, a phase that has high Lu/Hf but only slightly low Sm/Nd. Sequestration of such a phase would retard the radiogenic ingrowth of ^{176}Hf in the residual mantle without affecting ^{143}Nd significantly. Ca-perovskite is one mineral that could cause such a fractionation (Fig. 4b). Thus, one possibility is that Ca-perovskite accumulation at high pressure (lower mantle pressures) during differentiation of the Hadean magma ocean resulted in a complementary upper mantle with anomalously low Lu/Hf (Caro et al., 2005); in other words, the thick red line rotates clockwise. However, we can also see from Fig. 4c that an identical effect can also be generated by isolating the last dregs of the magma ocean laden with a magnetite component with high Lu/Hf (see Fig. 2b). Sequestering a Hadean residual liquid with high Lu/Hf would drive the remaining part of the mantle towards low Lu/Hf at a given Sm/Nd. It is clear that both low (this study) and high pressure (Caro et al., 2005) fractionation processes in a magma ocean could act together or separately to decouple Hf and Nd isotopes during Earth's early history.

4.2. High Pb

Sequestration of a Hadean matte might also have implications for the U/Pb systematics of the mantle. Based on Pb isotopic systematics, the bulk silicate Earth appears to have a time-integrated U/Pb ratio much higher than chondritic values, requiring that a significant amount of Pb was removed from the bulk silicate Earth. One possibility is that the building blocks of Earth were already volatile depleted in Pb, more so than any known chondrite meteorite groups.

Another possibility is that a significant amount of Pb has been sequestered in the Earth's core from the very beginning. However, Pb is not a particularly siderophile element but is instead chalcophile. Thus, if Pb is indeed in the core, sulfide segregation in addition to Fe metal segregation must have occurred. Additional sulfide segregation has been suggested to have occurred shortly after 99% of the core had already formed (Allegre et al., 1995; Frost et al., 2004; Wood and Halliday, 2005) or over Earth's history after core formation (see Hart and Gaetani (2006) for discussion). Sequestration of a Hadean matte formed during the very last stages of magma ocean crystallization might have contained Fe-oxides, sulfides, and Pb akin to our Proterozoic Fe–O–S magma (Fig. 2a and c). This matte would have sunk to the core-mantle boundary taking a significant component of Pb out of the bulk silicate Earth.

4.3. Radiogenic ^{187}Os but low Pt/Os

Additional geochemical imbalances may be resolved. The Fe–O–S sills have high Re but almost no initial Os (Fig. 5a), which translates into high ^{187}Re/^{188}Os. A Hadean matte with this signature would develop very radiogenic ^{187}Os/^{188}Os over ~4.5 Gy due to decay of ^{187}Re ($t_{1/2}$ ~ 42 Gy), such that even small amounts of contamination of a modern plume by this Hadean matte could give rise to hotspot magmas with high ^{187}Os. Radiogenic Os in some hotspot magmas has so far been interpreted to represent contamination by ancient recycled oceanic crust (Hauri and Hart, 1993; Eiler et al., 1996). However, the discovery of ^{186}Os/^{188}Os anomalies associated with decay of long-lived ^{190}Pt ($t_{1/2}$–490 Gy) in Hawaiian hotspot magmas has given rise to an another hypothesis: hotspot magmas have been contaminated by material from the liquid outer core, which has developed high Pt/Os and Re/Os ratios due to preferential retention of Pt and Re as the inner core solidified (Brandon et al., 1998; Brandon and Walker, 2005). Due to the very low isotopic abundances and very slow decay of ^{190}Pt, the fractionation of Pt/Os required to generate measurable deviations in ^{186}Os/^{188}Os over the course of Earth's history must be much larger than the fractionation of Re/Os (Brandon et al., 2003). Some of our Proterozoic Fe–O–S sills have super-chondritic Pt/Os ratios (Fig. 5b), but the fractionations are not high enough to yield the high ^{186}Os/^{188}Os observed in various hotspot magmas (Brandon et al., 2003). In particular, the Pt/Re ratios of our samples are too low to explain the high ^{186}Os to ^{187}Os observed in hotspot magmas (Brandon et al., 2003). Thus, although contamination by a Hadean matte can explain the radiogenic ^{187}Os in hotspot magmas, the Hadean matte should not have significant radiogenic ^{186}Os anomalies unless it has subsequently interacted with the outer core.

4.4. Thoughts on absolute abundances and the heat producing elements

We now return to the issue of absolute abundances. Without a massive regional investigation of the region affected by contact metamorphism and metasomatism, we simply cannot estimate the original trace-element contents of the Fe–O–S magmas. Nevertheless, the carbonate country rock affected by fluid metasomatism emanating from the Fe–O–S sills appear to be slightly enriched in Fe, resulting in a slight orangish tinge on weathered surfaces in the field. These rust-colored limestones appear to extend at least ~50–75 m away from the sills, which are each about 1 m in thickness. Assuming that these limestones have the same concentrations of incompatible trace elements seen in the one limestone we studied and that all of these trace elements originated from the Fe–O–S sills, it is possible that the original concentration of elements, such as Nd, Pb, Th, and U, in the sills could have been more than an order-of-magnitude higher than presently measured in the sills. While this estimate is admittedly crude, we know that

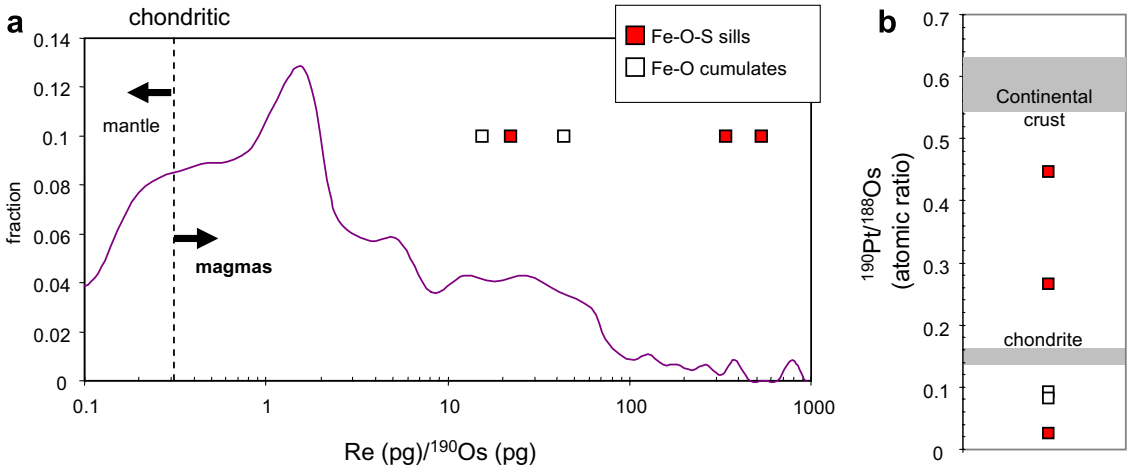

Fig. 5. (a) The weight ratios of Re (ppb) to ^{190}Os (ppb) for the magnetite samples plotted in comparison to a *logarithmic* histogram of Re/^{190}Os weight ratios from a literature compilation of different rocks, ranging from ultramafics to crustal and sedimentary lithologies (data were binned logarithmically). ^{190}Os was used rather than total Os because the Os in the magnetites has a very large radiogenic component (^{187}Os) from decay of ^{187}Re and as such its atomic weight deviates strongly from typical Os. Note that the magnetite samples have some of the highest Re/^{190}Os ratios. (b) ^{190}Pt/^{188}Os (atomic ratio) for Fe–O–S sills and Fe–O cumulates along with estimates of chondrite and average upper continental crust.

the trace-element concentrations in our Fe–O–S magmas are minimum estimates of the original concentrations. As such, it is possible that the Fe–O–S magmas could represent a significant repository for U and Th. We note, however, that neither the metasomatized carbonate nor the Fe–O–S magmas are enriched in K, another important heat-producing element. It is well-known that apatite-bearing Fe–O–S magmas are often enriched in K as well as U and Th (Kolker, 1982), begging the question of whether the Fe–O–S magmas in our study lost K or simply never had it.

5. IMPLICATIONS AND SPECULATIONS

While the Proterozoic Fe–O–S sill examined here is clearly not a perfect analog of residual liquids formed by magma ocean crystallization, our samples provide of means of testing whether Fe-rich liquids *of any kind* have the necessary trace-element composition to satisfy certain apparent global imbalances in trace-elements. Our analog could have been inconsistent with the magma ocean hypothesis, but we showed that this Proterozoic material indeed has the necessary composition to satisfy many global geochemical imbalances (U/Pb, Sm/Nd, Lu/Hf and Re/Os) that appear to be difficult to satisfy using upper mantle silicate fractionation. This lends support to the hypothesis that Fe-rich liquids, in the form of Fe-oxides and sulfides, might actually have formed early in Earth's history. However, as discussed above, the Fe-oxides and sulfides do not appear to be a sink for all of the heat-producing elements (K). If the global imbalances of U, Th, and K is associated with the global imbalances of U/Pb, Sm/Nd-Lu/Hf, and Re/Os ratios, a silicate or fluid component rich in K, U, Th and other highly incompatibles must accompany the Fe–O–S liquids. Such a component could be analogous to the KREEP (high K, rare-earth elements, and phosphorous) component in lunar basalts, which has been suggested to involve considerable amounts of apatite (McKay and Weill, 1977; Kolker, 1982; O'Neill, 1991a). Additional investigation of other Fe-rich magmas thus seems warranted.

In any case, we conclude that enough global geochemical imbalances can be potentially resolved by permanently sequestering a Fe–O–S magma. For purposes of speculation, we thus assume that a Hadean Fe-rich residual liquid did exist. If so, what would have been its fate after it sank to the core-mantle boundary? One possibility is that it was quickly assimilated into the core, removing any physical evidence of the Hadean matte's existence. Another possibility is that it has since remained at the core-mantle boundary because its density is intermediate between the metallic core and the silicate mantle. Such a layer could be detectable as follows. Although the elastic moduli of magnetite are known at pressures greater than 25 GPa (Haavik et al., 2000; Reichmann and Jacobsen, 2004), we note that the shear modulus of magnetite is low compared to upper mantle magnesian silicates (Reichmann and Jacobsen, 2004), qualitatively suggesting that a magnetite layer at the core-mantle boundary might have a low shear wave velocity. Even if the Hadean matte had mixed and reacted with mantle silicates, a low shear wave velocity is predicted because because Fe-rich post-perovskite silicate phases have been shown to have substantially lower shear velocities compared to the upper side of the ULVZ (Mao et al., 2006). A further drop in shear wave velocity may occur if this Hadean matte is also partially molten (Fig. 3b). At upper mantle pressures, the melting temperatures of the Fe–O system drops by ~600 °C when S is added (Naldrett, 1989). If S has a similar effect on freezing-point depression at high pressures, a zone of partial melting might be expected at the very base of the mantle. Thus, regardless of what form the Hadean matte is in, low shear wave velocities are predicted and this is consistent with the presence of the ULVZ.

How much of these putative Hadean Fe-oxides might now rest at the core-mantle boundary? Assuming a magma ocean with a primitive-mantle-like major element composition (~8 wt% FeO; McDonough and Sun (1995)), a very crude estimate of its mass can be had by considering a simple fractional crystallization model, wherein the enrichment of an element in a crystallizing melt (C^{m}) relative to its starting composition (C^{m0}) is given by $C^{m}/C^{m0} = F^{D-1}$ (where F is the remaining melt fraction and D is the effective weighted average partition coefficient of the element between the bulk crystallizing phases and the melt, i.e., the concentration in crystals divided by that in melt). We then consider how much crystal fractionation is required to increase the total FeO content of the magma ocean from ~8 to ~60 wt% total FeO. If the crystallizing phases are roughly in the proportion of 55% olivine, 25% orthopyroxene, 15% clinopyroxene and 5% plagioclase and the weighted average D for FeO is ~0.70 (we take $D_{olivine} \sim 0.9$, $D_{orthopyroxene} \sim D_{clinopyroxene} \sim 0.5$, $D_{plagioclase} = 0$; Walter (1998)), a residual melt fraction of $F \sim 0.13\%$ results. If the magma ocean represented the entire mantle (4×10^{24} kg), this would yield a ~2–5 km thick layer of pure Fe-oxide (assuming a Fe-oxide density of ~7000 kg/m^3) at the core-mantle boundary. This number should only be taken as an order of magnitude estimate because the real fractionation process is much more complicated, but given that we do not know the details of crystallization, a more sophisticated approach is not warranted for this paper. The ULVZ is believed to be 10–50 km thick (Garnero et al., 1998) and our estimated thickness is only slightly lower.

In conclusion, the promising trace-element signatures of the Fe–O–S sills investigated here support (but do not prove) the hypothesis (Boyet and Carlson, 2005; Tolstikhin and Hofmann, 2005) that a Fe-rich and incompatible trace element-enriched residual liquid could have formed during crystallization of the Hadean magma ocean and that this material sank to the bottom of the mantle, residing there indefinitely. However, many questions remain unanswered. What is the detailed petrogenetic origin of the Fe–O–S sills studied here? Was there some component of liquid immiscibility in their genesis (Philpotts, 1982)? Do these Fe-rich magmas sequester K, U and Th? If a Hadean Fe-rich layer rests on top of the core, to what extent does it facilitate or frustrate chemical reaction between the core and the silicate mantle? For example, even though we do not predict the Hadean matte to have high Pt/Os ratio and hence high $^{186}Os/^{188}Os$, could high ^{186}Os be attained by exchange of Os between the outer core and the Hadean matte? Could

this lead to decoupling between $^{186}Os/^{188}Os$ and Fe/Mn ratios (Humayun et al., 2004)? Finally, what is the viscosity of this layer? Could it be a high density but low viscosity layer as might be expected of a partially molten Fe–O–S layer? If so, to what extent does such a layer influence the initiation of thermal plumes rising from the base of the mantle (Jellinek and Manga, 2002)? How much of the Hadean matte could be entrained into plumes?

ACKNOWLEDGMENTS

This research was supported by NSF grants to Lee and Lenardic, a Packard Fellowship to Lee, and NASA grants to Yin. Discussions with V. Bennett, A. Brandon, R. Carlson, G. Caro, M. Hirschmann, S.D. Jacobsen, W. Mao, S. Mackwell, F. Nimmo, M.G. Little, W.P. Leeman, and F. Niu were helpful but we take blame for any biases. The inspiration for this paper came from a weekly reading group at Rice, which included D. Nunes, J. Hawthorne, J. Homburg, U. Horodyskyj, Z.-X. A. Li, S. Mackwell, and A. Maloy in addition to the authors. Discussions with Davis students B. Jacobsen, J. Naliboff, and C.S. Natrajan are also appreciated. We thank J. Li and anonymous reviewers for critical but constructive comments.

APPENDIX A. ANALYTICAL DETAILS

A.1. Trace element analyses

Samples were first crushed and powdered using a ceramic spex mill. Most trace elements were analyzed by inductively coupled plasma mass spectrometry (ICP-MS) by referencing to an external rock standard (USGS basalt standards BHVO1 and BIR1 with reference values from (Eggins et al., 1997)). An aliquot of sample powder (~0.05 g) was precisely weighed and then attacked for 24 h at 115 °C in sealed screw-cap teflon beakers using a mixture of 0.25 mL each of concentrated Seastar HF and $HClO_4$. The contents were then subjected to open beaker dry down at 170 °C, and the entire procedure was repeated once more. After the second dry down, 2 mL of 2 wt% Seastar HNO_3 was added to the chlorate residue, heated under sealed conditions to 100 °C, and ultrasonicated. This solution was then diluted up to ~100 mL and a pure Indium solution was added to the final diluted volume to achieve a final In solution concentration of 1 ppb. External rock standards and procedural blanks were prepared in the same way as samples. Solutions were free-aspirated through an Elemental Scientific Teflon nebulizer (10 μL/min uptake) into a ThermoFinnigan Element 2 single collector magnetic sector ICP-MS at Rice University. Most trace elements were determined using low mass resolution mode ($m/\Delta m = 300$) in order to maximize sensitivity (2 MHz/ppb In) and because most trace elements did not suffer major isobaric interferences. For those elements that potentially suffer from isobaric interferences (Mg, Fe, Ca, Na, K, P, Al, Sc, V), measurements were done in medium mass resolution ($m/\Delta m = 3000$). Some sensitivity was sacrificed but because these elements are major or minor elements, the decrease in sensitivity was negligible or even desired (in order to not saturate the detector). Concentrations were determined by first correcting all raw measurements (including the procedural blank) for instrumental drift by normalizing to the first measurement using the spiked In as a internal standard. Drift-corrected measurements were then corrected for blank contributions and then normalized to external standard measurements to yield actual rock concentrations (Table A.1).

A.2. Rhenium and osmium

Re and Os analyses required some degree of pre-concentration due to their low abundances in most rocks. Approximately 1 g of powdered sample was precisely weighed and added to a quartz glass vessel along with pre-weighed amounts of enriched ^{185}Re and ^{190}Os tracer solutions, which were calibrated against various known standards at Rice. This sample-spike mixture was frozen using a dry ice–ethanol bath and to this mixture was added 2 mL of concentrated HNO_3 and 1 mL of concentrated HCl. The glass vessel was sealed, placed in a sealed and metal cylinder for protection, and then heated at 230 °C for 72 h. Os was extracted using $CHCl_3$ solvent extraction and then microdistilled into a pure form. The remaining acid solution was centrifuged, dried down, and then taken up in 0.1 N HCl. The solution was then passed through 6 mL of AG150x-8 (100–200 mesh) cation exchange resin to strip off major cations. Os was introduced into the ICP-MS as a stable species in 0.1 N HCl. Concentrations were calculated from the measured $^{192}Os/^{190}Os$ ratio and that of the spike and normal. Re concentrations were similarly determined from the measured $^{187}Re/^{185}Re$ ratios (^{187}Os interferences on the Re splits were negligible as all Os was lost during processing of Re splits). Os and Re concentrations are accurate to the 1% level. Blank corrections were negligible (procedural blanks for Os were 2 pg and those for Re were 9 pg).

A.3. Platinum, iridium, and ruthenium

These elements were difficult to extract in the same chemical procedures used for Re and Os extraction. This was because of the very high Fe contents in the samples, which interfered with exchange column chemistry. In addition, it was very difficult to prevent oxidation of Fe into the insoluble Fe^{3+} state. This resulted in loss of Pt, Ir, and Ru by precipitation onto Fe-oxyhydroxides. For these elements, we resorted to NiS fire assay techniques. In a double-lined 15 mL ceramic crucible, approximately 0.5 g of rock powder was mixed with 6–8 g of a pre-mixed flux of NiS and borax and a mixed enriched isotope tracer solution (^{99}Ru, ^{198}Pt, ^{193}Ir) was added. The crucible and its contents were covered with snug cap and placed in a muffle furnace, first at 700 °C for 20 min, then at 1100 °C for 30 min. The crucible was then removed (while still hot) and allowed to quench in air. The NiS bead, containing the platinum group elements, was manually extracted and then dissolved in 6.7 N HCl at 130 °C. The entire solution was then filtered through 0.45 micron cellulose nitrate filters and the filtrate discarded. The platinum group element sulfides are not soluble in 6.7 N HCl and are caught by the filter paper. The filter paper was then dissolved completely with 16 N HNO_3 in a savillex beaker, then dried down and taken up

Table A.1

	LOD	USGS basalt standards		Wallrock carbonate M	Fe–O–S sill (magnetite-sulfide)			Fe–O cumulate (magnetite)	
		BHVO1	BHVO1		LS1	L2	L3	BSNEB	Tal
wt%									
Na_2O	0.0007	2.24	2.32	0.00072	0.0070	0.0041	0.0038	0.0536	0.0276
MgO	0.0002	7.94	8.07	20.6	0.670	1.92	1.77	6.78	3.17
Al_2O_3	0.00009	13.61	14.08	0.263	0.266	0.535	0.298	1.66	1.07
P2O5	0.0002	0.269	0.276	0.0115	0.00321	0.0032	0.00371	0.00078	0.00035
K_2O	0.001	0.514	0.525	0.0508	0.1349	0.0326	0.0177	<LOD	<LOD
CaO	0.0004	10.99	11.76	28.5	14.4	8.25	6.23	2.19	0.952
TiO_2	0.0003	2.73	2.80	0.013	0.008	0.014	0.010	0.192	0.046
FeO(t)	0.0005	10.82	11.17	1.80	58.03	65.51	65.22	57.61	69.68
ppm									
Li	0.006	4.89	4.96	2.76	4	5.38	6.24	13	7.38
Be	0.02	1.09	1.11	0.495	0.878	0.63	0.87	1.59	0.572
Sc[a]	0.004	32.1	32.4	0.403	0.227	0.343	0.277	4.39	0.464
Ti	0.3	16280	16830	83.9	45.9	83.8	60.4	1126	266
V[a]	0.02	303	326	10.4	37.2	17.8	57.2	8.84	6.22
Cr	4	286	294	11.3	36.7	21.1	12.9	41.1	27.9
Co[a]	0.02	44.1	44.6	6.78	215	107	212	48.3	81.9
Mn[a]	0.9	1331	1328	3587	667	1000	1168	646	464
Ni[a]	0.02	116	116	3.75	3.86	16.6	20.7	23.9	55
Cu	0.08	137	144	12.5	250	94.7	336	1.49	10.3
Zn[a]	0.6	100	109	131	167	282	279	199	734
Ga	0.01	21	21.7	0.664	2.81	2.54	1.77	7.96	8.31
Ge	0.03	2.8	2.89	0.195	6.12	6.95	7.09	6.38	7.48
Rb	0.003	9.13	9.47	2.73	3.69	2.3	3.21	1.11	0.299
Sr	0.006	386	405	73.3	62.2	28.9	55.1	6.86	11.3
Y	0.002	27.5	28.1	7.19	7.77	4.81	3.69	7.47	1.31
Zr	0.005	178	184	8.56	4.78	7.91	5.71	69.7	25.5
Nb	0.001	17.8	18.4	0.309	0.499	0.567	0.722	2.52	1.5
Cs	0.0002	0.0978	0.102	0.0854	0.0475	0.201	0.668	0.242	0.0799
Ba	0.009	131	136	6.69	3.42	2.16	3.09	3.19	1.67
La	0.001	15.2	15.8	1.66	2.1	1.37	1.05	0.308	0.221
Ce	0.001	37.0	38.8	3.61	4.49	2.75	2.27	1.04	0.549
Pr	0.0004	5.18	5.46	0.418	0.503	0.32	0.251	0.17	0.0777
Nd	0.001	24.4	25.1	1.78	2.22	1.43	1.09	0.878	0.406
Sm	0.001	6.02	6.21	0.465	0.497	0.339	0.245	0.312	0.146
Eu	0.0005	2.06	2.14	0.0941	0.0493	0.0375	0.02	0.0672	0.0257
Gd	0.0005	6.26	6.39	0.549	0.631	0.428	0.313	0.405	0.15
Tb	0.0002	0.958	0.982	0.0991	0.102	0.0681	0.0505	0.0795	0.0236
Dy	0.0007	5.27	5.46	0.734	0.698	0.456	0.338	0.674	0.153
Ho	0.0001	0.966	0.996	0.208	0.202	0.126	0.0936	0.218	0.0356
Er	0.0005	2.48	2.58	0.735	0.722	0.447	0.333	0.812	0.109
Tm	0.0001	0.334	0.345	0.127	0.127	0.0776	0.0565	0.147	0.0175
Yb	0.001	2.01	2.08	0.795	0.791	0.504	0.355	1	0.121
Lu	0.0002	0.271	0.28	0.128	0.119	0.0805	0.0543	0.199	0.0236
Hf	0.0007	4.13	4.27	0.145	0.0679	0.134	0.0885	1.6	0.434
Ta	0.0005	1.12	1.16	0.0192	0.0135	0.0384	0.0257	0.17	0.0891
Tl	0.0007	0.0594	0.0588	0.0366	0.0601	0.0308	0.0301	0.0153	0.009
Pb	0.006	2.21	2.2	8.79	69.3	94.6	83.6	1.06	1.77
Th	0.0006	1.23	1.28	2.03	0.983	0.951	0.709	2.42	2.62
U	0.0002	0.410	0.429	1.01	0.703	0.78	0.444	1.54	3.25
^{190}Os (ng/g)					0.012	0.062	0.141	0.088	0.051
Re (ng/g)					6.34	2.1	3.14	1.36	2.23
Pt(ng/g)					0.278	0.083	0.190	0.423	0.216
W (ng/g)					108	26.6	119	12.7	3.88
$Re/^{190}Os$ (weight ratio)					529	340	22.2	15.4	43.6
$^{187}Re/^{188}Os$ (atomic ratio)					2540	1633	107	74	209
$^{190}Pt/^{188}Os$ (atomic ratio)					0.45	0.27	0.026	0.093	0.082

[a] Determined on ICP-MS using medium mass resolution (all others determined in low resolution); LOD, limit of detection based on 3 times the standard deviation of the background.

in 0.1 N HCl. This solution was then passed through 2 mL of cation exchange resin (Bio-Rad AG50x-8, 100–200 mesh) to remove Ni and other interfering cations. The solution was then analyzed directly by ICP-MS. Procedural blanks were 2, 1 and 40 pg per gram of flux for Ru, Ir, and Pt (for 7 g flux used, this translates to *total* procedural blanks of 14, 7, and 280 pg, respectively).

A.4. Tungsten

Tungsten was determined here by directly measuring W/Re ratios and multiplying by Re concentrations determined by isotope dilution on independent aliquots. One aliquot was subjected to an HF–HNO_3 digestion, followed by an HNO_3–HCl digestion. The final dry down was taken up in 10 mL of 2% HNO_3. This diluted volume was not subjected to any further chemical treatments and was aspirated directly into the ICP-MS. The 187/184 mass ratio, which corresponds to the $^{187}Re/^{184}W$ ratio, was directly measured. Assuming that the Re/W ratio is not significantly fractionated in the plasma or mass spectrometer (this is reasonable as the two elements have similar masses, similar geochemical behaviors, and similar ionization efficiencies).

APPENDIX B. CALCULATION OF DENSITY

Densities at elevated pressures and temperatures were calculated following methods described in (Bina and Helffrich, 1992). The approach was to first integrate elastic properties and molar volumes to the elevated temperature of interest but at a constant reference pressure (1 atm). These molar volumes and elastic properties were then integrated up to the pressure of interest by solving the third order Birch–Murnaghan equation of state using a Newton–Raphson root finding technique. Elastic properties for magnetite (Fe_3O_4) were adopted from (Reichmann and Jacobsen, 2004): isothermal bulk modulus at 0 pressure $K_{0T} = 180$ GPa and $dK_T/dP = 5.2$ and an STP density of 5196 kg/m^3. A thermal Grüneisen ratio γth of 1.87 was adopted for conversion of adiabatic bulk moduli to isothermal bulk moduli (see (Reichmann and Jacobsen, 2004) for discussion). A 1 atm temperature-dependent thermal expansion coefficient from (Fei, 1995) was assumed.

REFERENCES

Allegre C. J., Manhes G., and Göpel C. (1995) The age of the Earth. *Geochim. Cosmochim. Acta* **59**, 1445–1456.

Anders E., and Grevesse N. (1989) Abundances of the elements: meteoritic and solar. *Geochim. Cosmochim. Acta* **53**, 197–214.

Ashwal L. D. (1982) Mineralogy of mafic and Fe–ti oxide-rich differentiates of the Marcy anorthosite massif, Adirondacks, New York. *Am. Mineral.* **67**, 14–27.

Barton M. D., and Johnson D. A. (1996) Evaporitic-source model for igneous-related Fe oxide-(REE-Cu-Au-U) mineralization. *Geology* **24**, 259–262.

Barton M. D., and Johnson D. A. (2000) Alternative brin sources for Fe-oxide(-Cu–Au) systems: implications for hydrothermal alteration and metals. In *Hydrothermal Iron Oxide Copper-gold and Related Deposits: A Global Perspective* (ed. T. M. Porter). Australian Mineral Foundation, pp. 43–60.

Bateman A. M. (1951) The formation of late magmatic oxide ores. *Econ. Geol.* **46**, 404–426.

Becker T. W., Kellog J. B., and O'Connell R. J. (1999) Thermal constraints on the survival of primitive blobs in the lower mantle. *Earth Planet. Sci. Lett.* **171**, 351–365.

Bennett V. C. (2003) Compositional evolution of the mantle. *Treatise Geochem.* **2**, 493–519.

Bennett V. C., Nutman A. P., and McCulloch M. T. (1993) Nd isotopic evidence for transient highly-depleted mantle reservoirs in the early history of the Earth. *Earth Planet. Sci. Lett.* **119**, 299–317.

Bina C. R., and Helffrich G. R. (1992) Calculation of elastic properties from thermodynamic equation of state principles. *Annu. Rev. Earth Planet. Sci.* **20**, 527–552.

Bizzarro M., Baker J. A., Haack H., Ulbeck D., and Rosing M. G. (2003) Early history of Earth's crust-mantle system inferred from hafnium isotopes in chondrites. *Nature* **421**, 931–933.

Blichert-Toft J., and Albarède F. (1997) The Lu-Hf isotope geochemistry of chondrites and the evolution of the mantle-crust system. *Earth Planet. Sci. Lett.* **148**, 243–258.

Boehler R., Chopelas A., and Zerr A. (1995) Temperature and chemistry of the core-mantle boundary. *Chem. Geol.* **120**, 199–205.

Bowring S. A., and Housh T. (1995) The Earth's early evolution. *Science* **269**, 1535–1540.

Boyet M., and Carlson R. W. (2005) ^{142}Nd evidence for early (>4.53) global differentiation of the silicate Earth. *Science* **309**, 576–581.

Brandon A. D., and Walker R. J. (2005) The debate over core-mantle interaction. *Earth Planet. Sci. Lett.* **232**, 211–225.

Brandon A. D., Walker R. J., Morgan J. W., Norman M. D., and Prichard H. M. (1998) Coupled 186Os and 187Os evidence for core-mantle interaction. *Science* **280**, 1570–1573.

Brandon A. D., Walker R. J., Puchtel I. S., Becker H., Humayun M., and Revillon S. (2003) ^{186}Os-^{187}Os systematics of Gorgona Island komatiites: implications for early growth of the inner core. *Earth Planet. Sci. Lett.* **206**, 411–426.

Bunge H.-P., Richards M. A., and Baumgardner J. R. (1996) Effect of depth-dependent viscosity on the planform of mantle convection. *Nature* **379**, 436–438.

Calzia J., Frisken J. G., Jachens R. C., McMahon A. B., and Rumsey C. M. (1988) Mineral resources of the Kingston Range Wilderness Study area, San Bernardino County, California. *U.S. Geol. Survey Bull.* **1709-C**, 21.

Carlson R. W. (1994) Mechanisms of Earth differentiation. *Rev. Geophys.* **32**, 337–361.

Caro G., Bourdon B., Wood B. J., and Corgne A. (2005) Trace-element fractionation in Hadean mantle generated by melt segregation from a magma ocean. *Nature* **436**, 246–249.

Dobson D. P., and Brodholt J. P. (2005) Subducted banded iron formations as a source of ultralow-velocity zones at the core-mantle boundary. *Nature* **434**, 371–374.

Dziewonski A., and Anderson D. L. (1981) Preliminary reference Earth model. *Phys. Earth Planet. Int.* **25**, 297–356.

Eggins S. M., Woodhead J. D., Kinsley L., Mortimer G. E., Sylvester P., McCulloch M. T., Hergt J. M., and Handler M. R. (1997) A simple method for the precise determination of >40 trace elements in geological samples by ICP-MS using enriched isotope internal standardisation. *Chem. Geol.* **134**, 311–326.

Eiler J. M., Farley K. A., Valley J. W., Hofmann A. W., and Stolper E. M. (1996) Oxygen isotope constraints on the sources of Hawaiian volcanism. *Earth Planet. Sci. Lett.* **144**, 453–468.

Einaudi M. T., and Burt D. M. (1982) Introduction, terminology, classification and composition of skarn deposits. *Econ. Geol.* **77**, 745–754.

Fei Y. (1995) Thermal expansion. In *Mineral Physics and Crystallography*, Vol. Reference Shelf 2, American Geophysical Union, pp. 29–44.

Frost D. J., Liebske C., Langenhorst F., McCammon C. A., Tronnes R. G., and Rubie D. C. (2004) Experimental evidence for the existence of iron-rich metal in the Earth's lower mantle. *Nature* **428**, 409–412.

Garnero E. (2000) Heterogeneity in the lowermost mantle. *Ann. Rev. Earth Planet. Sci.* **28**, 509–537.

Garnero E., Revenaugh J., Williams Q., Lay T., Kellogg L. H., Gurnis M. Wysession M. E., Knittle E., and Buffet B. A. (1998) The core-mantle boundary region. American Geophysical Union, pp. 319–334.

Grand S. P. (1994) Mantle shear structure beneath the Americas and surrounding oceans. *J. Geophys. Res.* **99**, 11591–11621.

Haavik C., Stolen S., Fjellvag H., Hanfland M., and Hausermann D. (2000) Equation of state of magnetite and its high-pressure modification: thermodyanmics of the Fe–O system at high pressure. *Am. Mineral.* **85**, 514–523.

Hart S. R., and Gaetani G. A. (2006) Mantle Pb paradoxes: the sulfide solution. *Contrib. Mineral. Petrol.*. doi:10.1007/s00410-006-0108-1.

Hauri E. H., and Hart S. H. (1993) Re-Os isotope systematics of HIMU and EMII oceanic island basalts from the south Pacific Ocean. *Earth Planet. Sci. Lett.* **114**, 353–371.

Heaman L., and Grotzinger J. P. (1992) 1.08 Ga diabase sills in the Pahrump Group, California: implications for development of the Cordilleran miogeocline. *Geology* **20**, 637–640.

Hess P. C., and Parmentier E. M. (1995) A model for the thermal and chemical evolution of the Moon's interior: implications for the onset of mare volcanism. *Earth Planet. Sci. Lett.* **134**, 501–514.

Hewett D. F. (1948) Iron deposits of the Kingston Range, San Bernardino County, California. *Calif. Div. Mines Geol. Bull.* **129**, 193–206.

Hofmann A. W. (1988) Chemical differentiation of the Earth: the relationship between mantle, continental crust, and oceanic crust. *Earth Planet. Sci. Lett.* **90**, 297–314.

Hofmann A. W., and White W. M. (1982) Mantle plumes from ancient oceanic crust. *Earth Planet. Sci. Lett.* **57**, 421–436.

Horn I., Foley S. F., Jackson S. E., and Jenner G. A. (1994) Experimentally determined partitioning of high field strength- and selected transition elements between spinel and basaltic melt. *Chem. Geol.* **117**, 193–218.

Humayun M., Liping Q., and Norman M. (2004) Geochemical evidence for excess iron in the Hawaiian mantle: implications for mantle dynamics. *Science* **306**, 92–94.

Jacobsen S. B., and Wasserburg G. J. (1979) The mean age of mantle and crustal reservoirs. *J. Geophys. Res.* **84**, 7411–7427.

Jang Y. D., and Naslund H. R. (2003) Major and trace element variation in ilmenite in the Skaergaard intrusion: petrologic implications. *Chem. Geol.* **193**, 109–125.

Jang Y. D., Naslund H. R., and McBirney A. R. (2001) The differentiation trend of the Skaergaard intrusion and the timing of magnetite crystallization: iron enrichment revisited. *Earth Planet. Sci. Lett.* **189**, 189–196.

Jellinek A. M., and Manga M. (2002) The influence of a chemical boundary layer on the fixity, spacing and lifetime of mantle plumes. *Nature* **418**, 760–763.

Johnson K., Barnes C. G., Browning J. M., and Karlsson H. R. (2002) Petrology of iron-rich magmatic segregations associated with strongly peraluminous trondhjemite in the Cornucopia stock, northeastern Oregon. *Contrib. Mineral. Petrol.* **2002**, 564–581.

Kellogg L. H., Hager B. H., and van der Hilst R. D. (1999) Compositional stratification in the deep mantle. *Science* **283**, 1881–1884.

Kolker A. (1982) Mineralogy and geochemistry of Fe–Ti oxide and apatite (Nelsonite) deposits and evaluation of the liquid immiscibility hypothesis. *Econ. Geol.* **77**, 1146–1158.

Lee C.-T. A., Leeman W. P., Canil D., and Li Z.-X. A. (2005) Similar V/Sc systematics in MORB and arc basalts: implications for the oxygen fugacities of their mantle source regions. *J. Petrol.* **46**, 2313–2336.

Mao W. L., Mao H. K., Sturhahn W., Zhao J., Prakapenka V. B., Meng Y., Shu J., Fei Y., and Hemley R. J. (2006) Iron-rich post-perovskite and the origin of ultralow-velocity zones. *Science* **312**, 564–565.

McBirney A. R. (1975) Differentiation of the Skaergaard intrusion. *Nature* **253**, 691–694.

McDonough W. F., and Sun S.-S. (1995) The composition of the Earth. *Chem. Geol.* **120**, 223–253.

McKay G. A., and Weill D. F. (1977) KREEP petrogenesis revisited. *J. Geophys. Res.*, 2339–2355.

Menard J.-J. (1995) Relationship between altered pyroxene diorite and the magnetite mineralization in the Chilean Iron Belt, with emphasis on the El Algarrobo iron deposits (Atacame region, Chile). *Mineralium Deposita* **30**, 268–274.

Murakami M., Hirose K., Kawamura K., Sata N., and Ohishi Y. (2004) Post-perovskite phase transition in $MgSiO_3$. *Science* **304**, 855–857.

Naldrett A. J. (1989) *Magmatic sulfide deposits*. Oxford University Press, New York, 186 p.

O'Neill H. S. C. (1991a) The origin of the Moon and the early history of the Earth-a chemical model. Part 1: the Moon. *Geochim. Cosmochim. Acta* **55**, 1135–1157.

O'Neill H. S. C. (1991b) The origin of the Moon and the early history of the Earth—a chemical model. Part 2, the Earth. *Geochim. Cosmochim. Acta* **55**, 1159–1172.

O'Nions R. K., Evensen N. M., and Hamilton P. J. (1979) Geochemical modeling of mantle differentiation and crustal growth. *J. Geophys. Res.* **84**, 6091–6101.

Osborn E. F. (1959) Role of oxygen partial pressure in the crystallization and differentiation of basaltic magma. *Am. J. Sci.* **257**, 609–647.

Philpotts A. R. (1967) Origin of certain iron-titanium oxide and apatite rocks. *Econ. Geol.* **62**, 303–315.

Philpotts A. R. (1982) Compositions of immiscible liquids in volcanic rocks. *Contrib. Mineral. Petrol.* **80**, 201–218.

Reichmann H. J., and Jacobsen S. D. (2004) High-pressure elasticity of a natural magnetite crystal. *Am. Mineral.* **89**, 1061–1066.

Rudnick R. L., Gao S. (2004) Composition of the continental crust. In *Treatise of Geochemistry*, Vol. 3 (eds. H. D. Holland and K. K. Turekian), pp. 1–64.

Stegman D. R., Jellinek A. M., Zatman S. A., Baumgardner J. R., and Richards M. A. (2003) An early lunar core dynamo driven by thermochemical mantle convection. *Nature* **421**, 143–146.

Tolstikhin I., and Hofmann A. W. (2005) Early crust on top of the Earth's core. *Phys. Earth Planet. Int.* **148**, 109–130.

van der Hilst R. D., Widiyantoro S., and Engdahl E. R. (1997) Evidence for deep mantle circulation from global tomography. *Nature* **386**, 578–584.

Vervoort J. D., and Blichert-Toft J. (1999) Evolution of the depletd mantle: Hf isotope evidence from juvenile rocks through time. *Geochim. Cosmochim. Acta* **63**, 533–556.

Vervoort J. D., and Patchett P. J. (1996) Behavior of hafnium and neodynium isotopes in the crust: constraints from Precambrian crustally derived granites. *Geochim. Cosmochim. Acta* **60**(19), 3717–3733.

Walter M. J. (1998) Melting of garnet peridotite and the origin of komatiite and depleted lithosphere. *J. Petrol.* **39**, 29–60.

Walter M. J., and Tronnes R. G. (2004) Early Earth differentiation. *Earth Planet. Sci. Lett.* **225**, 253–269.

Williams Q., and Garnero E. J. (1996) Seismic evidence for partial melt at the base of the mantle. *Science* **273**, 1528–1530.

Wood B. J., and Halliday A. N. (2005) Cooling of the Earth and core formation after the giant impact. *Nature* **437**, 1345–1348.

Wood J. A., Dickey J. S., Marvin U. B., and Powell B. N. (1970) Lunar anorthosites. *Science* **167**, 602–604.

Wookey J., Stackhouse S., Kendall J.-M., Brodholt J. P., and Price G. D. (2005) Efficacy of the post-perovskite phase as an explanation for lowermost-mantle seismic properties. *Nature* **438**, 1004–1007.

Wysession M. E., Lay T., Revenaugh J., Williams Q., Garnero E. J., Jeanloz R., and Kellogg L. H. The D″ discontinuity and its implications. In *The core-mantle boundary region* (eds. M. Gurnis M. E. Wysession E. Knittle and B. A. Buffet). American Geophysical Union, pp. 273–297.

Associate editor: Alan D. Brandon